Asian Journal of Chemistry; Vol. 32, No. 11 (2020), 2773-2777

ASIAN JOURNAL OF CHEMISTRY

https://doi.org/10.14233/ajchem.2020.22708

Effect of Nickel Concentration in Natural Zeolite as Catalyst in Hydrocracking Process of Used Cooking Oil

E.P. SUSI[1], K. WIJAYA[1,*], WANGSA[1], R.A. PRATIKA[1] and P.L. HARIANI[2]

[1]Physical Chemistry Laboratory, Department of Chemistry, Universitas Gadjah Mada, Yogyakarta-55281, Indonesia
[2]Faculty of Mathematics and Natural Science, Universitas Sriwijaya, Jalan Palembang-Prabumulih Km 32 Indralaya, Sumatera Selatan, Indonesia

*Corresponding author: E-mail: karnawijaya@ugm.ac.id

Received: 4 March 2020; *Accepted*: 16 July 2020; *Published online*: 28 October 2020; AJC-20100

Nickel impregnated zeolites were successfully synthesized through wet impregnation using activated natural zeolites (ANZs) and the nickel nitrate hexahydrate ($Ni(NO_3)_2{\cdot}6H_2O$) precursor at different concentrations of 1%, 2% and 3% (w/w) (hereafter referred to as ANZ/Ni 1%, ANZ/Ni 2%, and ANZ/Ni 3%). The synthesized products were characterized using X-ray diffraction (XRD), Fourier transform infrared spectroscopy (FTIR), surface area analyzer (SAA), scanning electron microscopy (SEM), total acidity measurements by employing ammonia adsorption and Brunauer-Emmett-Teller (BET) theory. The obtained catalysts were employed in the hydrocracking of waste cooking oils, and the formed products were analyzed through gas chromatography-mass spectrometry (GC-MS). The FTIR results indicated that impregnated of ANZs with Ni can increase zeolite acidity. The test results of total acidity revealed that 3% ANZ/Ni catalyst exhibited the maximum total acidity of 3.70 mmol/g. XRD diffractogram confirmed the successful impregnation of Ni into ANZs, which was indicated by the characteristic diffraction peaks appearing at 2θ of 9.75º, 13.41º, 19.56º, 22.25º, 25.61º, 27.66º and 31.91º. SEM analysis indicated that the particle size of zeolite catalysts was non-uniform, but these catalysts exhibited a highly uniform surface after they were activated. Moreover, the ANZ catalysts impregnated with different concentrations of Ni exhibited a highly uniform particle size. The ANZ/Ni 3% catalyst has small uniform particles. The BET results revealed that the ANZ/Ni 2% catalyst exhibited the maximum pore volume and surface area and relatively smaller radii of pores. GC-MS was employed to determine liquid products, and its results showed that the ANZ/Ni 3% catalyst had the maximum amount of liquid products of 18%.

Keywords: Zeolites, Ni-impregnated, Catalyst, Waste cooking oil, Hydrocracking.

INTRODUCTION

Zeolites are the most vital catalysts in chemical industries especially in the petroleum industry. They exhibit suitable catalytic properties partly because of their uniform pore size, crystalline framework, strong acidity and high internal surface area [1]. Natural zeolite is one of the most abundant natural materials in Indonesia especially in West Java (Tasikmalaya, Bogor and Sukabumi), Central Java (Klaten and Wonosari) and East Java (Bayah) [2]. Natural zeolites contain a large amount of impurities, thereby necessitating their modification and activation to enhance catalytic activities. Impregnation has become a recommended method to increase the active sites of catalysts. In catalyst systems, transition metals can serve as active catalyst sites during hydrocracking. Acidity levels substantially influences catalyst performance. A higher catalytic acidity leads to more active sites, which can generate adsorption energy for reactants, thereby increasing the amount of cracked feeds [3].

Nickel is a eco-friendly and has considerable hydrogenation activity [4], therefore easily forms covalent coordination bonds to facilitate intermediate production on the surface of catalysts. Catalyst-reactant bonds are weak; thus, reaction products were easily separate from the catalyst surface. Hence, the reaction accelerates, even when the product contains long carbon chains. Thus, nickel can serve as a promising metal for increasing the acidity of zeolites through wet impregnation to synthesize catalysts by adsorbing precursor salts that provide the active components of Ni in their solution. The increase in the zeolite acidity results in regular structural changes, which increase the effectiveness and selectivity of zeolites [4].

By using the catalyst, a catalyst activity test was performed for the hydrocracking of cooking oil, which was already used,

This is an open access journal, and articles are distributed under the terms of the Attribution 4.0 International (CC BY 4.0) License. This license lets others distribute, remix, tweak, and build upon your work, even commercially, as long as they credit the author for the original creation. You must give appropriate credit, provide a link to the license, and indicate if changes were made.

into biogasoline. The used cooking oil is an abundant source of the raw materials of biodiesel. These raw materials contain large amounts of fatty acids; can be easily acquired from household, industrial, and commercial disposed products at a low cost, and are available in large quantities [5]. Additionally, used cooking palm oil contains palmitic acid, oleic acid, stearic acid, linoleic acid, lauric acid and myristic acid [6]. Therefore, this oil can be promisingly cracked into a short hydrocarbon that can serve as a fuel. From used materials, vegetable oils, energy crops, aquatic biomass, and forest products, biogasoline can be manufactured. Currently, method development for biogasoline generation is commonly achieved through processes, such as hydrocracking and thermal cracking, which produce large portions of biogasoline [7,8]. This study reported the influence of nickel impregnation on natural zeolites to explore their applications in the hydrocracking of the used cooking oil into biogasoline because zeolites provide high selectivity and activity during cracking to achieve maximal production of the expected fraction of biogasoline (C5-C12).

EXPERIMENTAL

The materials used in this study were Klaten natural zeolite, used cooking oil, 37% HCl, nickel nitrate hexahydrate, silver nitrate, and 25% ammonia (NH_3) from Merck. Nitrogen and hydrogen gases were obtained from PT. Samator Gas Industri, Indonesia.

Activation of natural zeolites: Initially, natural zeolites were washed with distilled water and dried at 120 ºC for 12 h. Natural zeolites were activated by employing 9 M HCl at 90 ºC and for 2 h. Then, the resulting product was washed using distilled water to remove Cl^- ions and was tested using 0.1 M $AgNO_3$ to ensure complete removal. Subsequently, at 550 ºC, natural zeolites were calcined for 5 h to acquired activated natural zeolites, which then were analyzed through XRD and FTIR.

ANZ/Ni Fabrication through wet impregnation: Activated natural zeolites (ANZs) were impregnated with varying concentrations of $Ni(NO_3)_2{\cdot}6H_2O$ (1%, 2% and 3%). Impregnation was achieved by stirring for 24 h at room temperature. Moreover, ANZ/Ni was dried at 120 ºC. The dried ANZ/Ni was calcined using N_2 gas flow at 550 ºC for 3 h. Subsequently, by using H_2 gas, reduction was then conducted at 400 ºC for 3 h to acquire ANZ/Ni 1%, ANZ/Ni 2% and ANZ/Ni 3%. All catalysts were analyzed using XRD, FTIR, BET, SAA, SEM and the acidity test.

Hydrocracking of used cooking oil: The used cooking oil was catalytically and thermally hydrocracked at 450 ºC for 1 h at the ratio of catalyst to feed of 1:100. Hydrocracking was performed under a hydrogen gas flow of 20 mL min^{-1}. By using GC-MS, the composition of liquid products was explored. From the hydrocarbon fraction with the carbon atoms of C5-C12, the biogasoline fraction was calculated.

RESULTS AND DISCUSSION

FTIR studies: The activation of natural zeolites resulted dealumination, *i.e.*, removal of aluminium from the framework of zeolites, thereby increasing the Si/Al zeolite ratio. IR spectra show an increase in the intensity at the wavelengths of 794 and 462 cm^{-1}, which corresponded to Si-O (Fig. 1a). This increase resulted from an increase in the Si-O (quartz) group. Moreover, the acid treatment increased the hydrophobic nature of natural zeolites because of the increased hydrophobic Si-O groups. The decrease in the intensity of the wavenumber 3425 cm^{-1} corresponding to O-H group indicated the increase in hydro-phobic properties. Furthermore, intensity decreased at the 1635 cm^{-1}, which showed the O-H bending vibration [9,10].

To increase their acidity, activated natural zeolites were impregnated using nickel. FTIR spectra present the difference between Ni (1%, 2%, and 3%) impregnated zeolites and ANZ in terms of their adsorption band at 3425 cm^{-1} (Fig. 1b). This change was caused by the decreased number of -OH groups. The acidic capacity of zeolites enhanced because of photons production caused by water molecule separation that was related to the Brønsted acid sites of zeolites [11,12]. An intensity change at 794 cm^{-1} is observed in the FTIR spectra. The

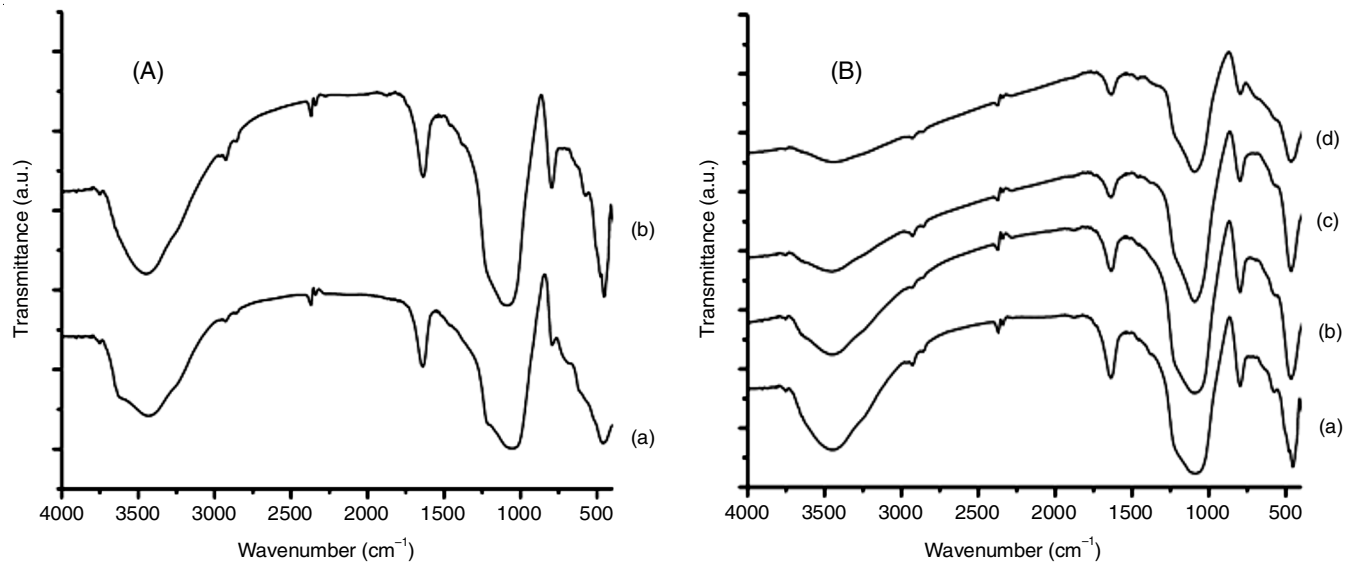

Fig. 1. FTIR spectra of (A) NZ (a), ANZ (b) and (B) ANZ (a), ANZ/Ni 1% (b), ANZ/Ni 2% (c), ANZ/Ni 3% (d)

higher was the Ni-impregnation concentration, the wider was the adsorption band at a higher wavenumber. These results revealed that Ni addition can change the vibrations of Si-O group in zeolites.

XRD studies: After activation, the crystallinity of natural zeolites was analyzed to determine the impact of the acid treatment on the crystal framework of natural zeolites. Fig. 2a illustrates the diffractograms of natural zeolites acquired before and after they were activated through the acid treatment. Dealumination using the acid treatment can change the Si/Al ratio and acidity of natural zeolites. The obtained diffractogram indicates that main components of natural zeolites were mordenite and clinoptilolite, which remained mixed with quartz. The activation results indicated that zeolites can maintain their crystallinity without any substantial damage [13].

Fig. 2b presents the XRD pattern of Ni-impregnated (1%, 2%, and 3%) zeolites and activated natural zeolites. The XRD results showed no considerable changes in diffractogram for all zeolites, indicating successful impregnation of nickel into activated natural zeolite. Characteristic diffraction peaks appearing at 2θ of 13.41º, 19.56º, 22.25º, 25.61º, 27.66º and 31.91º indicated ANZ purity [14]. After impregnation, no new peaks were obtained, and the resulting NZ and ANZ-Ni catalyst diffractograms were similar, which indicated that the Ni metal impregnated into zeolite framework did not substantially change its original crystal structure and synthesis was successful.

Acidity: For all zeolites, the acidity test was conducted using the ammonia adsorption gravimetric method. The acidity test results showed an increase in acidity with an increase in the Ni concentration. The 3% ANZ-Ni catalyst exhibited the maximum total acidity of 3.70 mmol g^{-1} (Table-1). The acidity level of 1% and 2% AZN-Ni catalysts was lower than that of ANZ, because of the agglomeration of the nickel metal loaded on natural zeolite, which led to the zeolite acid site blocking. The acidity of zeolites was generated from silanol groups present within the zeolite framework [15]. The total acidity increased because of nanopore dimension formation caused by nickel, which increased the number of active silanol sites, thereby increasing the number of Brønsted acid sites in the zeolite materials [16].

TABLE-1
ACIDITY TEST FOR EACH CATALYST

Sample	Acidity
NZ	2.98
ANZ	3.54
ANZ-Ni 1%	3.14
ANZ-Ni 2%	3.52
ANZ-Ni 3%	3.70

The FTIR spectra of ANZs, NZs and Ni-impregnated (1%, 2% and 3%) zeolites acquired using NH_3 adsorption gravimetric method, *i.e.*, through interaction with NH_3 (after acidity test), revealed a new adsorption peak at 1404-1396 cm^{-1}. This adsorption peak corresponded to NH_4^+ asymmetric stretching vibrations [9]. No large difference between the amounts of adsorbed NH_3 in ANZs and Ni-impregnated zeolites was observed.

SEM studies: Fig. 3 presents the SEM results of ANZs, NZs and Ni-impregnated (1%, 2%, and 3%) zeolites. The natural zeolites catalysts contained non-uniform crystals while the ANZ catalysts exhibited an impurity-free clean surface and small uniform particles. The smaller was the size of particles, the more effective was hydrocracking for liquid biogasoline production. Zeolites impregnated with different concentrations of nickel had smaller and more uniform crystalline shape than ANZ had, which indicated the good dispersion of nickel particles. This phenomenon resulted from agglomeration. The presence of nickel led to stronger interactions that induced crystal structure expansion [7]. The higher concentrations of nickel led to more uniform size of catalyst particles. No large nickel particles were observed on the catalyst surface, which indicated that ANZ-Ni 3% catalyst was effective to be used as a zeolite supporting material in hydrocracking for biogasoline production.

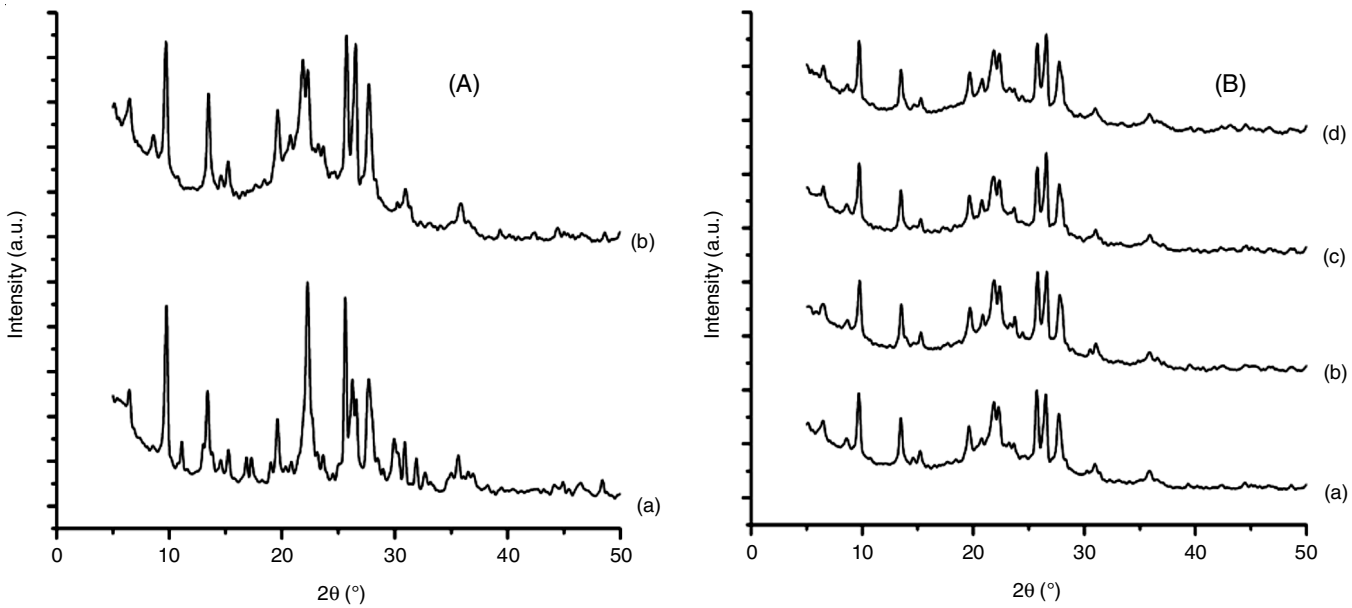

Fig. 2. XRD patterns of (A) NZ (a), ANZ (b) and (B) ANZ (a), ANZ/Ni 1% (b), ANZ/Ni 2% (c), ANZ/Ni 3% (d)

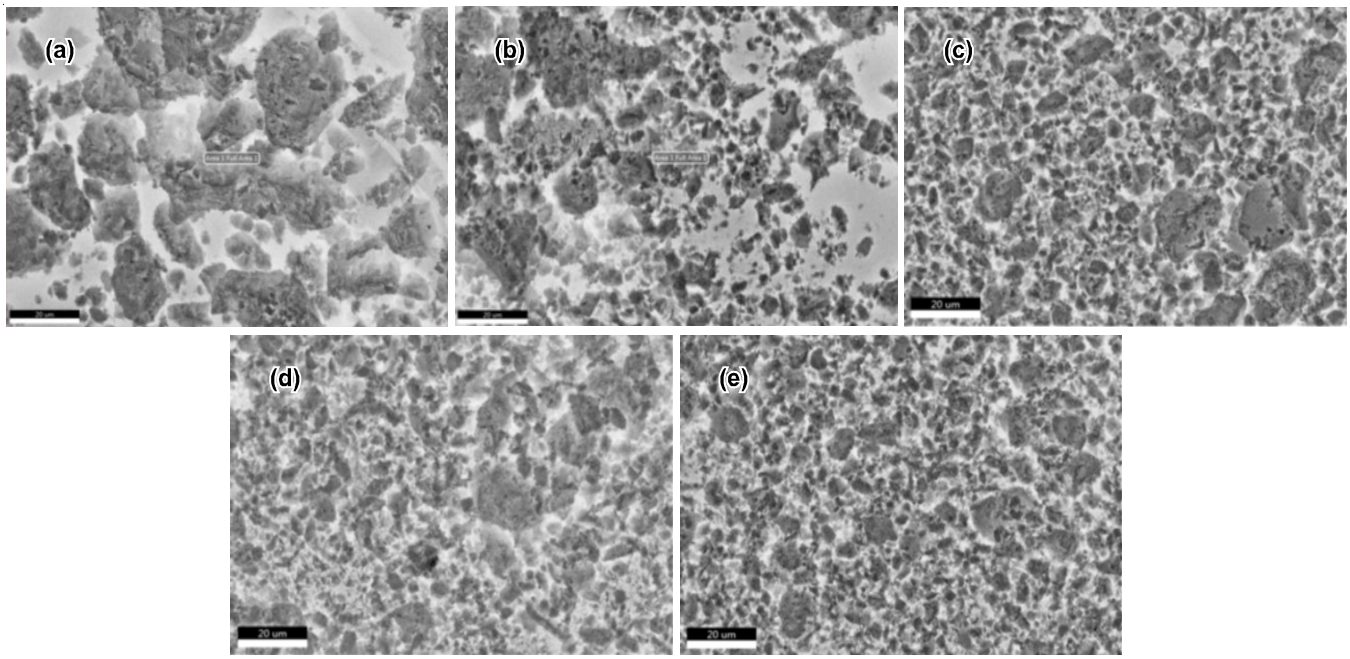

Fig. 3. SEM images of (a) NZ, (b) ANZ, (c) ANZ/Ni 1%, (d) ANZ/Ni 2% and (e) ANZ/Ni 3%

BET studies: Catalysts were characterized using BET to determine their pore average size, specific surface area and pore volume. The BET results (Table-2) indicated that the pore size and specific surface area of ANZ catalysts were higher than those of natural zeolite catalysts. This phenomenon was caused by the activation treatment. Due to a high adsorption capacity, the pore volume of catalysts decreased. With Ni (ANZ-Ni 1%) impregnation, the catalyst surface area decreased, but its pore volume and pore size increased. The surface area of ANZ-Ni 2% increased and this catalyst exhibited the highest pore volume and surface area. However, it had low pore radii. ANZ-Ni 3% exhibited a relatively smaller pore volume and surface area but had larger pores. This phenomenon was caused by the restructuring of zeolites during calcination. Some Ni atoms were adhered to pore walls, thereby rendering the pore size smaller. When the total pore volume and pore size increased and decreased, respectively, nickel adhered to the surface of zeolites through aggregate formation, which led the surface and pore volume to widen and increase, respectively [11,13].

TABLE-2
SPECIFIC SURFACE AREA, AVERAGE PORE SIZE, AND TOTAL PORE VOLUME OF CATALYST

Sample	Specific surface area (m^2/g)	Average pore size (θ)	Total pore volume (cc/g)
NZ	14.9059	11.273	8.4018
ANZ	93.6341	22.974	1.0756
ANZ-Ni 1%	31.6221	45.374	7.1741
ANZ-Ni 2%	56.9626	29.636	8.4407
ANZ-Ni 3%	51.5128	32.175	8.2872

For the used cooking oil, thermal hydrocracking provided more conversion of liquid products than catalytic hydrocracking (Table-3). During catalysis, nickel-impregnated zeolite generated larger amounts of liquid products than NZ and ANZ catalysts did, and ANZ/Ni 3% catalyst was the optimum for liquid product generation, which provided 18% yield, because nickel served as the active site, Thus, it was relatively better to catalyze hydrocracking reactions and the results optimal. Furthermore, the high acidity value of ANZ/Ni 3% can increase the number of active sites, thereby rendering the hydrocracking of the used cooking oil conducted to produce biogasoline optimal [2,17].

TABLE-3
CONVERSION OF HYDROCRACKING PRODUCTS FROM EACH CATALYST

Catalyst	Liquid product conversion (%)
Thermal	22.2
NZ	13.31
ANZ	12.50
ANZ-Ni 1%	6.66
ANZ-Ni 2%	13.98
ANZ-Ni 3%	18.00

Conclusion

Nickel-impregnated zeolites were successfully synthesized and applied to produce biogasoline through the hydrocracking of the used cooking oil. The surface areas of the synthesized catalysts are larger than those of natural zeolites (NZs). The conversion of liquid products into biogasoline from the hydrocracking of the used cooking oil showed that ANZ/Ni 3% was the catalyst providing the maximum amount of liquid product of 18%.

ACKNOWLEDGEMENTS

This research was supported by grant of the Universitas Gadjah Mada fund for scientific research RTA (Rekognisi Tugas Akhir) 2019; No. 2129/UN1.DITLIT/DIT-LIT/LT/2019.

CONFLICT OF INTEREST

The authors declare that there is no conflict of interests regarding the publication of this article.

REFERENCES

1. S. Huang, X. Liu, L. Yu, S. Miao, Z. Liu, S. Zhang, S. Xie and L. Xu, *Micropor. Mesopor. Mater.*, **191**, 18 (2014); https://doi.org/10.1016/j.micromeso.2014.02.039
2. W. Sriningsih, M.G. Saerodji, W. Trisunaryanti, Triyono, R. Armunanto and I.I. Falah, *Procedia Environ. Sci.*, **20**, 215 (2014); https://doi.org/10.1016/j.proenv.2014.03.028
3. B. Purwono, C. Anwar and A. Hanapi, *Indones. J. Chem.*, **13**, 1 (2013); https://doi.org/10.22146/ijc.21318
4. A. Suseno, K. Wijaya, W. Trisunaryanti and R. Roto, *Orient. J. Chem.*, **34**, 1427 (2018); https://doi.org/10.13005/ojc/340332
5. A. Tangy, I.N. Pulidindi and A. Gedanken, *Energy Fuel*, **30**, 3151 (2016); https://doi.org/10.1021/acs.energyfuels.6b00256
6. N. Taufiqurrahmi, A.R. Mohamed and S. Bhatia, *Bioresour. Technol.*, **102**, 10686 (2011); https://doi.org/10.1016/j.biortech.2011.08.068
7. B. Liu, X. Cheng, J. Liu and H. Pu, *Fuel*, **223**, 1 (2018); https://doi.org/10.1016/j.fuel.2018.02.196
8. A. Ahmadi, D.D. Ganji and F. Jafarkazemi, *Energy Convers. Manage.*, **119**, 1 (2016); https://doi.org/10.1016/j.enconman.2016.07.061
9. K. Wijaya, D.A. Ani, T. Iqmal, S. Akhmad, A. Rachmat and Hasanudin, *Nano Hybrids Compos.*, **19**, 46 (2017); https://doi.org/10.4028/www.scientific.net/NHC.19.46
10. C. Ma, J. Geng, D. Zhang and X. Ning, *J. Energy Inst.*, **93**, 581 (2020); https://doi.org/10.1016/j.joei.2019.06.007
11. J. Cheng, Z. Zhang, X. Zhang, J. Liu, J. Zhou and K. Cen, *Int. J. Hydrogen Energy*, **44**, 1650 (2019); https://doi.org/10.1016/j.ijhydene.2018.11.110
12. M. Ebrahiminejad and R. Karimzadeh, *Adv. Powder Technol.*, **30**, 1450 (2019); https://doi.org/10.1016/j.apt.2019.04.021
13. C. Manrique, A. Guzmán, J. Pérez-Pariente, C. Márquez-Álvarez and A. Echavarría, *Micropor. Mesopor. Mater.*, **234**, 347 (2016); https://doi.org/10.1016/j.micromeso.2016.07.017
14. G. Cui, J. Wang, H. Fan, X. Sun, Y. Jiang, S. Wang, D. Liu and J. Gui, *Fuel Process. Technol.*, **92**, 2320 (2011); https://doi.org/10.1016/j.fuproc.2011.07.020
15. M.O. Kazakov, K.A. Nadeina, I.G. Danilova, P.P. Dik, O.V. Klimov, V.Y. Pereyma, E.Y. Gerasimov, I.V. Dobryakova, E.E. Knyazeva, I.I. Ivanova and A.S. Noskov, *Catal. Today*, **305**, 117 (2018); https://doi.org/10.1016/j.cattod.2017.08.048
16. P.P. Dik, G.G. Danilova, M.O. Kazakov, K.A. Nadiena, V. Budukva, P. Yu, O.V. Klimov, P.P. Prosvirin, E.Y. Gerasimov, T.O. Bok, E.E. Dobryakova, E.E. Knyazeva, I.I. Ivanova and A.S. Noskov, *Fuel*, **237**, 178 (2019); https://doi.org/10.1016/j.fuel.2018.10.012
17. Q. Cui, S. Wang, Q. Wang, L. Mu, G. Yu, T. Zhang and Y. Zhou, *Fuel*, **237**, 597 (2019); https://doi.org/10.1016/j.fuel.2018.10.040